

# Application of uniform design in optimisation of three stage ageing of Al–Cu–Mg alloys

N. Gao · M. J. Starink · N. Kamp · I. Sinclair

Received: 4 February 2006 / Accepted: 10 July 2006 / Published online: 28 February 2007  
© Springer Science+Business Media, LLC 2007

**Abstract** The hardness variations and precipitation behaviour during the three-stage ageing of three Al–Cu–Mg alloys were investigated using micro-hardness testing and differential scanning calorimetry (DSC). To facilitate the determination of an optimised heat treatment, a uniform design method was employed by which the influences of three-stage interrupted ageing on the hardness and precipitation can be elucidated with a limited number of experiments. It is found that optimised heat treatment with maximum hardness can be achieved for non-stretched materials by applying the method of three-stage ageing, but there is no obvious effect for stretched T351 materials. A long initial Stage I and a suitable Stage II ageing time are beneficial for hardness, and the Stage II ageing at 25 °C shows more beneficial effect than ageing at 65 °C. The hardness increase in Stage I and Stage III ageing is closely related to the S phase content.

## Introduction

Al–Cu–Mg based alloys (2xxx series) are widely used in structural applications, in particular alloys with

Cu:Mg atomic ratio close to 1 are used extensively in the aerospace sector [1, 2]. It is often thought that, once an aluminium alloy is artificially aged at an intermediate temperature (e.g. peak aged T6 temper at 180 °C), the microstructure and mechanical properties remain unchanged for an indefinite period at lower temperature. However, recent observations made on an Al–Cu–Mg alloy with a much lower solute content using positron annihilation spectroscopy have indicated that vacancies may remain mobile at room temperature after these alloys were first aged at 180 °C [3]. Such mobility will facilitate solute diffusion leading to possible further (secondary) precipitation at room temperature [4]. In fact, the subject of secondary ageing has been investigated for several aluminium alloys [5–8], and it has been shown that so-called secondary precipitation may occur in several aluminium alloys when an interrupted low temperature secondary ageing is introduced through a three stage ageing process [4, 9, 10]. This three stage ageing process is shown schematically in Fig. 1 and involves the following stages [4]:

- Solutionizing and quenching
- Stage I: Ageing at elevated temperature ( $T_A > 100$  °C) for a short period ( $t_A$ , 10 min–8 h), then quench to ambient temperature.
- Stage II: Ageing at low temperature ( $T_B$ , typically below 70 °C) for a long period ( $t_B$ , few hours to several weeks).
- Stage III: Ageing at elevated temperature ( $T_C = T_A$ ).

In Stage I,  $T_A$  is similar to the ageing temperature normally used for T6 tempers, and the ageing time for this stage ranges typically from 10 min to 8 h, depending on the specific alloy. After Stage I, the

N. Gao (✉) · M. J. Starink · N. Kamp · I. Sinclair  
Materials Research Group, School of Engineering Sciences,  
University of Southampton, Southampton SO17 1BJ, UK  
e-mail: N.Gao@soton.ac.uk

Present Address:

N. Kamp  
Manchester Materials Science Centre, UMIST, Manchester  
M1 7HS, UK

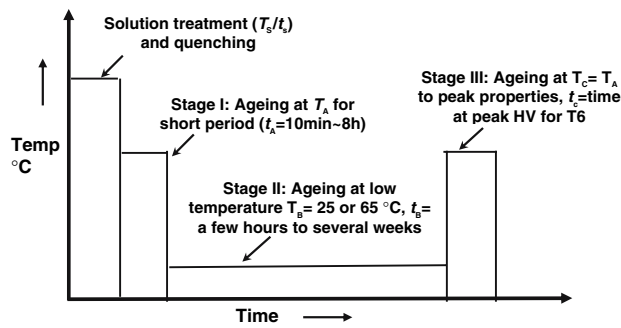


**Fig. 1** Schematic representation of the three stages of T6I6 interrupted ageing treatment

alloys are underaged and display hardness values 50–80% of those corresponding to a full T6 temper, which leaves potential for further precipitation to achieve a maximum hardness in the following Stage II and Stage III ageing. The alloys are then held (Stage II) for various periods at low temperature ( $T_B$ ). Finally,  $T_C$  in Stage III is usually taken close to  $T_A$ , and ageing is continued until peak hardness is reached. This complete treatment has been given the designation T6I6, signifying the standard T6 heat treatment is interrupted by a dwell period (I) at a lower temperature before resuming artificial ageing [4, 9]. Several reports indicated that selected T6I6 treated alloys demonstrated simultaneous improvements in hardness, tensile properties and fracture toughness ranging from 5 to 30%, depending on the composition and specific processing conditions [4, 8–10]. These beneficial effects of interrupted ageing are believed to emanate from secondary precipitation occurring during the dwell period which can nucleate finely dispersed precipitates in the final aged microstructure [9, 11].

Although the above experimental results have revealed that the selection of the parameters of the three stage ageing treatment is critical for the optimising of the heat treatment condition [4, 9], varying with different aluminium alloys, no report on the methodology for optimising selection of parameters in three stage heat treatment has been published. Little is known about the microstructure and hardness evolution in Stage I and Stage II. The objectives of this work are to further analyse the specific ageing response for different aluminium alloys by separately analysing the detailed hardness data of Stage I, II and III for three Al–Cu–Mg alloys. Differential scanning calorimetry (DSC) analysis was carried out to examine the precipitation reaction at different ageing stages. To optimise the process parameters of the three-stage heat treatment, a uniform design method was used.

## Experimental procedures

Three Al–Cu–Mg alloys have been studied and their compositions are gathered in Table 1. The composition of alloy B is close to the median composition of AA204. These alloys have been manufactured at QinetiQ, Farnborough, UK [12, 13]. Billets were conventionally cast, stress relieved, homogenized, hot rolled to 20 mm thickness, solution heat treated, cold water quenched, stretched by ~2.5% and then left at room temperature for a few months. Except for solution treatment temperatures, the processing was essentially the same for all alloys (optimum solution treatment temperatures for individual alloys were identified via determination of the start temperature of (incipient) melting using DSC [14]).

The grain structure of the alloys in as-received T351 condition was determined using electron backscatter diffraction (EBSD) on a JEOL JSM–6500 field emission gun scanning electron microscope (FEG-SEM) [15]. Selected samples were studied using transmission electron microscopy (TEM). Thin foils for TEM were prepared using a standard procedure: samples of 400  $\mu\text{m}$  thickness were punched, ground to 250  $\mu\text{m}$  and electro-polished using a 1/3 nitric acid, 2/3 methanol solution held at  $-20^\circ\text{C}$  to  $-30^\circ\text{C}$ , with a voltage of 25 V. TEM observation was performed at 200 kV using a JEOL JEM-2000FX.

A range of T6I6 treatments was conducted on the three alloys. Three dominant variables were chosen and studied systematically to optimise the heat treatment: (i) the initial Stage I ageing time,  $t_A$ , (ii) the Stage II interrupted low temperature ageing temperature,  $T_B$  and (iii) the Stage II ageing time,  $t_B$ . The other heat treatment parameters were taken as constant for each alloy including solution temperature/time ( $T_S/t_S$ ), initial and final ageing temperature ( $T_A$  and  $T_C$ ) and final ageing time ( $t_C$ ). The selection of these constant heat treatment parameters were based on previous experimental results [12, 16]. A uniform design method is employed in this study to replace the complete combination of experimental parameters by using relatively limited experiment trials uniformly distributed within the parameter space. These experimental trials are determined using the number-theoretic method

**Table 1** Chemical compositions of alloys (wt.%)

Alloy	Cu	Mg	Li	Zr	Mn
A	2.27	1.03	1.56	0.11	0.01
B	4.34	1.37	–	–	0.42
C	1.48	1.43	0.54	0.11	–

[17, 18], which was mathematically proved to be a good approximation of the complete combination of experimental parameters [19]. For each of the three variables (factors), different treatment levels were incorporated (Table 2). Because there are only two levels of variation (factor) selected for  $t_A$ , ten representative experiments were chosen by using the mix-level uniform design table  $U_{10}(5^2 \times 2^1)$  (or  $U_m(q_1^{S_1} \times q_2^{S_2})$ ), where  $U$  represents uniform design,  $m$  the total number of experiments,  $q_1, q_2$  the number of levels of each factor, and  $S_1, S_2$  the number of the factors. Therefore,  $U_{10}(5^2 \times 2^1)$  represents that there are a total 10 experiments, with three factors (two with 5 levels and one with 2 levels) in these experiments. The uniform design table  $U_{10}(5^2 \times 2^1)$  is given in Table 3 and the full matrix of experiment is detailed in Table 4.

$T_A = T_C = 190$  °C was chosen as previous work on these alloys indicated that a satisfactory balance in yield strength, fatigue crack growth resistance and formability can be achieved by ageing these alloys at 190 °C [2, 16]. Initial Stage I ageing time,  $t_A$  is specific to each alloy and was determined with the aid of strength predications using the model described in Ref. [20]. The Stage I and III ageing times,  $t_A$  and  $t_C$ , for alloys A and C were longer than for alloy B because it has been found that these two alloys took a longer time to reach peak hardness due to their Li addition [16]. All samples were solution treated at 513, 495 and 505 °C respectively for alloy A, B and C, and subsequently quenched into water at room temperature before further ageing treatments began. For comparison purposes, additional one-step ageing heat treatments have been carried out for the three alloys starting from both the T351 and the freshly quenched condition. Following earlier experiments, treatments at 190 °C for 15 h (for alloys A and C), and 6 h (for alloy B) were chosen, as these ageing times are known to result in peak hardness for single stage ageing at 190 °C [16, 21]. These treatments are here designated T351 + 190 °C and T6 temper, respectively.

Ageing response was studied by performing Vickers micro-hardness tests at different stages on surfaces

ground with #1200 grade SiC-paper. Four indentations were made on each specimen with a 1 kg load and a mean hardness is reported. The standard deviation (STDEV) is within 5% of experimental data for these testing samples. Thus accuracy of the hardness determinations is about  $4^{-1/2} \times 5\% = 2.5\%$ . Samples aged at different stages of T6I6 were studied by DSC in a Perkin–Elmer Pyris 1 calorimeter. Samples were discs (5 mm diameter and approximately 1 mm thickness) that were machined prior to heat treatment. Scanning over the temperature range 5–540 °C at a constant heating rate of 10 °C/min was performed. To correct for baseline drift and heat capacity of the sample and reference, a two-stage baseline correction was performed [14].

## Results and discussion

### Microstructure before ageing

All the alloys at the as-received T351 condition have a plate-shaped grain structure, although variations in recrystallization level and grain size are evident. EBSD maps of the grain structure for the three alloys are presented in Fig. 2, in which the higher angle grain boundaries (misorientations  $> 12^\circ$ ) are displayed by thick dark lines and low angle grain boundaries (misorientations 2 to  $12^\circ$ ) by thin grey lines. A (local) high concentration of low angle grain boundaries (such as seen for alloys A and C) is indicative of the presence of a subgrain structure induced by the rolling process which is retained due to recrystallisation during solution treatment being suppressed. Thus the Mn-containing alloy B is seen to be predominantly recrystallized with coarse grains (145  $\mu\text{m}$ ), whilst the Zr-containing alloys A and C were partially recrystallized with smaller grain sizes with average grain size of 8 and 40  $\mu\text{m}$ . TEM analysis reveals that the Zr containing alloy A contains many small sub-grains (Fig. 3) and there are many dislocation lines and loops for as-received T351 samples. The dislocations result from the stretching after solution treatment and the loops

**Table 2** The ageing parameters investigated

Parameter (factors)	Treatment level				
	1	2	3	4	5
Alloy	B/A = C	B/A = C	B/A = C	B/A = C	B/A = C
Stage I ageing time, $t_A$ (h)	1.0/2.5	2.0/5.0	2.5/6.3	3.0/7.5	4.0/10
Stage II ageing time, $t_B$ (h)	20	100	300	600	1200
Stage II ageing temperature, $T_B$ (°C)	25	65			

**Table 3** Uniform design table ( $U_{10}(5^2 \times 2^1)$ )

Experiment no.	Number of factors		
	$t_A$ (h)	$t_B$ (h)	$T_B$ (°C)
1	1	1	1
2	1	2	2
3	2	3	1
4	2	4	2
5	3	5	1
6	3	1	2
7	4	2	1
8	4	3	2
9	5	4	1
10	5	5	2

**Table 4** Heat treatment conditions for the 10 selected experiments guided by the uniform design table

Experiment no.	Stage I		Stage II		Stage III
	$T_A = T_C$ (°C)	$t_A$ (h) (A/B/C)	$t_B$ (h)	$T_B$ (°C)	$t_C$ (h) (A/B/C)
1	190	2.5/1.0/2.5	20	25	15/6.0/15
2	190	2.5/1.0/2.5	100	65	15/6.0/15
3	190	5.0/2.0/5.0	300	25	15/6.0/15
4	190	5.0/2.0/5.0	600	65	15/6.0/15
5	190	6.3/2.5/6.3	1200	25	15/6.0/15
6	190	6.3/2.5/6.3	20	65	15/6.0/15
7	190	7.5/3.0/7.5	100	25	15/6.0/15
8	190	7.5/3.0/7.5	300	65	15/6.0/15
9	190	10/4.0/10	600	25	15/6.0/15
10	190	10/4.0/10	1200	65	15/6.0/15

No. Variables (factors) investigated by the uniform design method in bold format

are generally caused by condensation of quenched in vacancies [13].

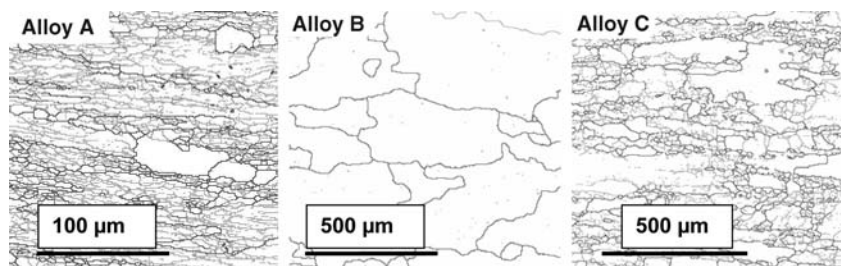
**Hardness tests**

Figure 4 shows the hardness results after the three stage of T6I6 ageing heat treatment. For alloy A, the No. 3–5 samples and the No. 8–9 samples show the highest hardness values. Among them, the No. 9 sample ( $t_A = 10/4.0/10$  h,  $T_B = 25$  °C, and  $t_B = 600$  h) demonstrates the highest hardness value compared

with the other heat treatments. A maximum of 9.2% increase in hardness can be seen from 120 Hv of the No. 2 sample to 131 Hv of the No. 9 sample. For alloy B, the No. 3 and the 5 samples have relatively high hardness values, but it is the No. 9 sample which possesses the highest hardness. A maximum of 7.8% increase in hardness has been achieved from the No. 1 (142 Hv) to the No. 9 (153 Hv) samples for the alloy B. The No. 4–5 samples provide relatively high hardness value for the alloy C, but still less than the No 9 sample, which shows a 7.1% increase in hardness compared with the No. 1, 2 and 8 samples. Overall, the No. 9 T6I6 treatment gives the best result for all the three alloys.

The influence of each stage on hardness variations is investigated in Figs. 5 and 6. Figure 5, in which the Stage I ageing time has been plotted against the Hv values collected after Stage I ageing, demonstrates that the hardness invariably increases with the increase of Stage I ageing time. Figure 6 shows the Stage II ageing time against hardness measured after Stage III. It can be seen that there are similar trends in the change of the final Stage III hardness for the alloys A and C during Stage II ageing between 25 °C and 65 °C. That is, in most cases, the Stage III hardness gradually increases with the increase of Stage II ageing time until 600 h, and then Stage III hardness starts to decrease. The same trend is seen for alloy B during the Stage II ageing at 25 °C, but not at 65 °C. In general, Stage II ageing for 600 h (No. 9 sample) always leads to the maximum hardness among the all of samples; and Stage II ageing at 25 °C mostly provides a higher hardness than ageing at 65 °C. The No. 9 treatment has the longest Stage I ageing time and the second longest Stage II ageing time, therefore, it can be concluded that a longer initial Stage I and Stage II ageing times ( $t_A$  and  $t_B$ ) are important. Figure 6 shows that increasing the Stage II (low temperature) ageing temperature to 65 °C does not produce better results than ageing at 25 °C. Considering that both No. 9 and No. 10 samples have the same Stage I ageing time, it is interesting to see that No. 9 sample has distinctly higher hardness than the No. 10 sample, though the

**Fig. 2** EBSD maps of TS sections of alloys A, B and C—showing higher angle grain boundaries (>12°) by dark lines and lower angle grain boundaries (2–12°) by grey lines



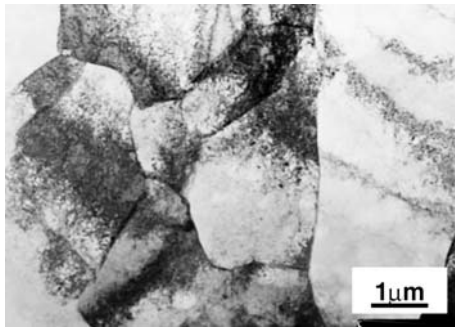


**Fig. 3** TEM micrograph of the alloy A at T351 condition

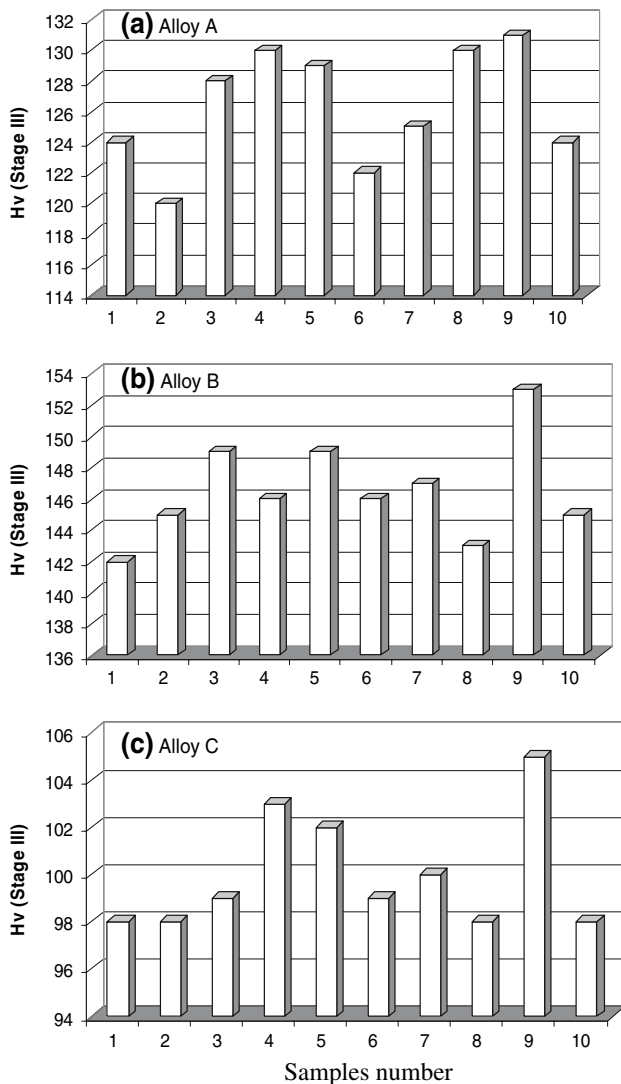


**Fig. 4** Comparison of Vickers hardness results from different T6I6 heat treatments for the three alloys

former has a shorter Stage II ageing time (600 h) than the latter (1200 h) but different Stage II ageing temperature, which means that Stage II ageing at 25 °C

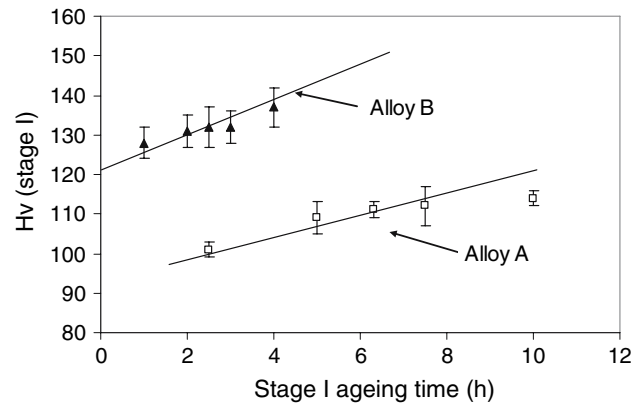


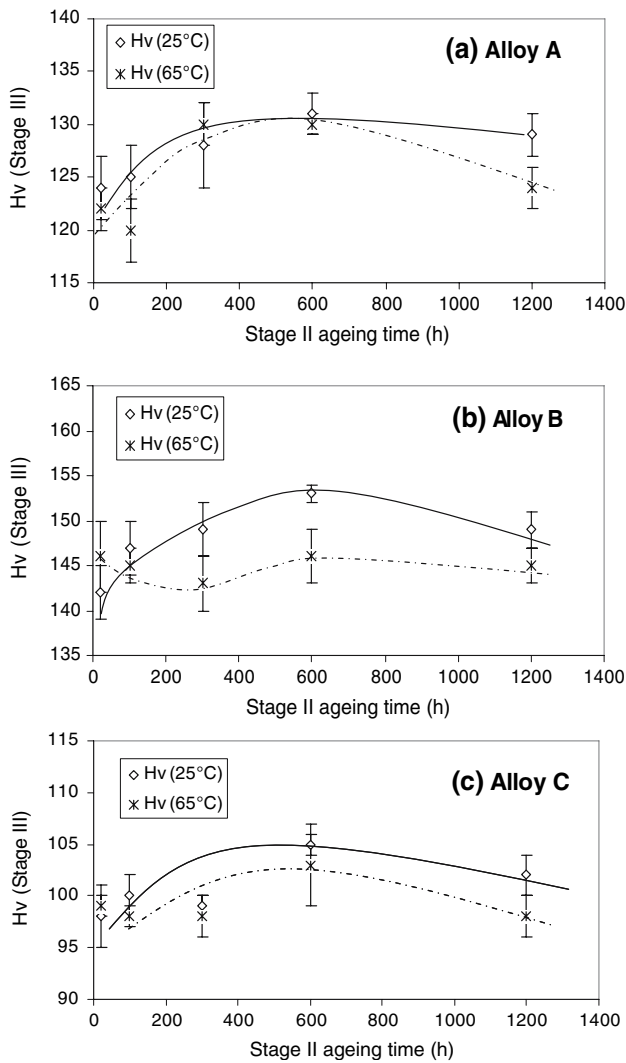
**Fig. 5** Effect of Stage I ageing time on Stage I Vickers hardness for alloys A and B

(No. 9) is more beneficial than at 65 °C (No. 10). It is possible that the lower hardness in the No. 5 sample (Stage II ageing at 25 °C/1200 h) is due to the reduction of Stage I ageing time (6.3/2.5/6.3) for the three alloys.

A comparison of the hardness values between the best T6I6 results (No 9. sample) and the results of one step ageing for T351 (T351 + 190 °C) and T6 tempers (solutionised and quenched plus 190 °C) is shown in Fig. 7. Figure 7 demonstrates that the hardness values of the No. 9 sample after three stage ageing are higher than the T6 temper for all of the three alloys, respectively increasing hardness by 6.5%, 10.1% and 9.4% for the alloys A, B and C. However, only the alloys A and C show a slight improvement of the harness after the No. 9 three stage ageing, compared with the one step aged T351 alloys, but there is no improvement in hardness for the alloy B. This indicates that the optimisation of the T6I6 three stage ageing heat treatment may be sensitive to alloy composition.

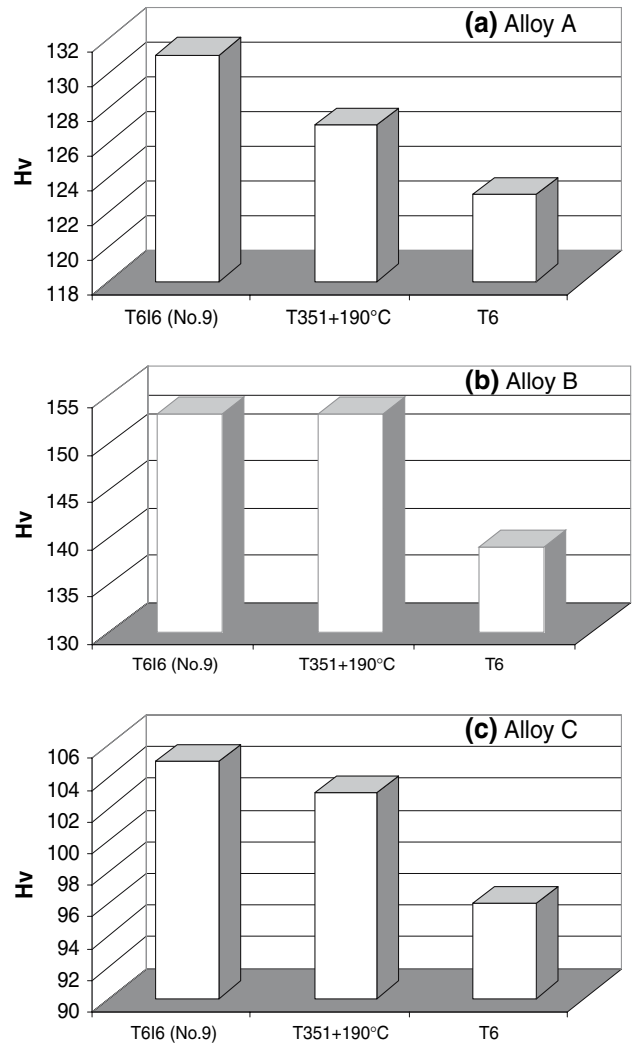
#### DSC analysis

Figure 8 shows the DSC curves of the alloys A, B and C before and after different stages of ageing for the No. 9 treatment. In general, solutionised and quenched samples have two exothermic peaks, one at 50–150 °C which is related to Cu–Mg co-cluster formation [1, 22], and another peak around 250–350 °C due to S formation. They also have two endothermic effects, at 150–250 °C and 350–480 °C, respectively due to zone/cluster dissolution and S dissolution [14, 23, 24]. After initial Stage I ageing, alloy A still shows a small exothermic peak around 100 °C from co-cluster formation, whilst this effect has disappeared entirely for alloys B and C. This may be due to a higher lithium content in



**Fig. 6** Effect of Stage II ageing time on Stage III Vickers hardness for the three alloys. (Note: the order of the samples numbers is different with the increase of Stage II ageing time due to the specific characteristics of the uniform design method.)

alloy A, compared with the alloys B and C, which delays the co-cluster precipitation process. The disappearance of the effect for alloys B and C implies that co-cluster formation has been completed during the Stage I of the ageing process. Compared with the solutionised and quenched condition, a substantial reduction of S formation peak after initial Stage I ageing indicates that substantial S phase has been formed during Stage I. The DSC curves demonstrate that the alloys are not stabilized after initial Stage I ageing, and further S precipitation follows in the subsequent ageing processes, especially in Stage III. The reduction of the S phase formation effect both in Stage I and Stage III (shown in Fig. 8) coincides with the increase of hardness (shown in Figs. 4–6), indicating



**Fig. 7** Comparison of Vickers hardness results between best result from T616 (No. 9 sample) and the results of one step ageing for T351 (T351 + 190 °C) and for fresh quenched alloys (T6 temper)

that the formation of S phase is responsible for the increase in hardness. It is expected that the precipitation process occurring in Stage II is mainly related to co-cluster formation [7]. This is supported by Fig. 8 (b and c), in which there are similar S peaks after Stage I and Stage II for both alloys B and C. However, it is not clear why the S peak shows a drop from Stage I to Stage II for alloy A, and why the Stage I is slightly lower than the Stage I + II in the DSC curves of alloy C, which need to be further investigated. It is possible that small uncertainties in the baseline of the DSC or small compositional variations between samples have caused some of the differences in the (apparent) magnitude of the S phase formation effects in Fig. 8.

A comparison of DSC curves of alloy B in T351 and T351 + 190 °C /6 h conditions, as well as after Stage I,

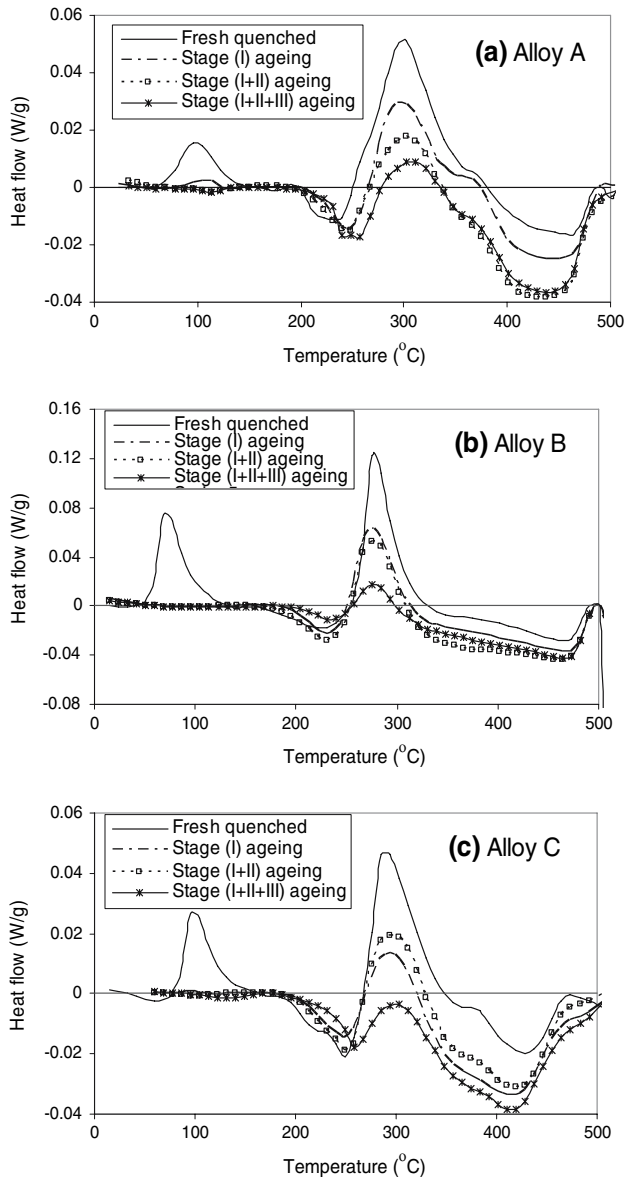


**Fig. 8** DSC curves of alloys A, B and C before and after different stages of ageing (No. 9 sample)

and Stage III for the No. 9 sample is shown in Fig. 9. Figure 9 reveals two apparent differences between them. Firstly, the S formation effect in the T351 sample (with peak at 257 °C) has moved to higher temperature in the three stage ageing samples (275 °C). This behaviour has been seen in other DSC works on similar aluminium alloys which shows that stretching by 2–3% after quenching causes the S precipitation peak to shift to a lower temperature [25]. This can be explained by the dislocations introduced by stretching, which accelerate the S precipitation. The dislocations act as preferential nucleation sites to facilitate heterogeneous nucleation of S phase and as short circuit

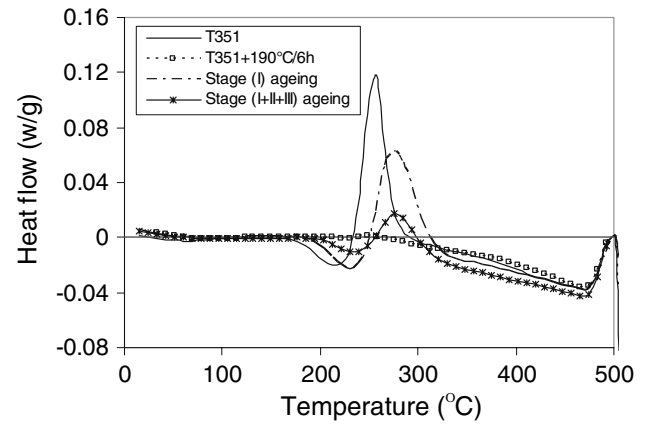


**Fig. 9** Comparison of DSC curves of alloy B between T351, T351 + 190 °C/6 h and after different stages of ageing (No. 9 sample)

diffusion paths along dislocation cores to accelerate the precipitation rates. Secondly, the S formation peak disappears very quickly for the T351 + 190 °C/6 h sample which means that S phase formation has been completed after 190 °C/6 h ageing. The 190 °C/6 h ageing also causes the co-cluster dissolution effect to disappear for the T351 sample. However, the S formation peak and co-cluster dissolution effect in the three stage ageing samples still exists, although the total accumulated ageing time of the three stage ageing at 190 °C already reaches up to 10 h for alloy B. This characteristic may be due to the rates of S phase precipitation and co-cluster dissolution being suppressed due to the immediate Stage I ageing of the T6I6 sample since one of the main differences for both samples is that ageing at 190 °C/6 h for the T351 sample commenced after quenching and a few months of natural ageing, and the T6I6 sample immediately started the Stage I ageing after solution and quenching. Similar behaviour has been found in an Al–Zn–Mg alloy [7] in which ageing at 150 °C after quenching plus 4 days at room temperature showed a distinct increase in hardening rate compared with ageing at 150 °C immediately after quenching. Also, work on an Al–Cu–Mg alloy demonstrated that on secondary natural ageing after 5 or 7 min at 190 °C, hardening takes place at a rate nine to 16 times slower than natural age hardening [26]. This behaviour has been suggested to be due to a slow release of vacancies from Cu-rich aggregates formed during the initial high temperature treatment [5, 26], which undergo a structural reorganization and possibly a change in composition, leading to species with a different thermal stability.

From the results of this study, it seems that the three stages of the T6I6 process indeed improve

hardness of quenched Al–Cu–Mg based alloys (without stretch), but not for T351 (quenched and stretched) alloys. This indicates that T6I6 and stretching are not complementary. Two reasons may be put forward to explain this: (1) Stretching reduces vacancy levels and provides heterogeneous precipitation sites; (2) Rapid heterogeneous precipitation in the Stage I ageing may limit driving force for low temperature precipitation, whilst low vacancy concentration will limit diffusivity. However, further analysis of stretched and unstretched alloys for T6I6 optimisation is clearly of interest for further work. Detailed microstructural analysis, such as APFIM (Atom Probe Field Ion Microscopy) and TEM, need to be conducted in order to more clearly explain the strengthening mechanism from the early precipitation phases through the T6I6 three stage ageing, especially to examine the fine precipitation which is claimed to be the main cause in improving the mechanical properties of alloys [9, 11].

## Conclusions

The uniform design method, micro-hardness and DSC have been applied together to investigate the hardness change and precipitation response of the individual stages of T6I6 temper for Al–Cu–Mg alloys.

1. The uniform design method is shown to be effective in optimising the variables of the studied three stage heat treatment for Al–Cu–Mg alloys.
2. The application of a T6I6 temper to these alloys indicates that it can increase the hardness by 7–9% as compared to the T6 temper (un-stretched), but there is no obvious beneficial effect for stretched T351 materials. The extent of improvement in hardness from the T6I6 three stage ageing heat treatment may be sensitive to alloy composition.
3. The selection of a long initial Stage I and a suitable Stage II ageing time is important. In the most cases, the Stage II ageing at 25 °C shows more beneficial effect than ageing at 65 °C.
4. DSC analysis indicates that the hardness increase in Stage I and Stage III ageing is closely related to the S phase content.

## References

1. Starink MJ, Gao N, Davin L, Yan J, Cerezo A (2005) *Phil Mag* 85:1395
2. Starink MJ, Gao N, Kamp N, Wang SC, Pitcher PD, Sinclair I (2006) *Mater Sci Eng A* 418:241
3. Somoza A, Dupasquier A, Polmear IJ, Folegali P, Ferragut R (2000) *Phys Rev B* 61:14454
4. Lumley RN, Polmear LJ, Morton AJ (2001) In: *Proceedings from Materials Solutions Conference*, 5–8 November. Indianapolis, IN, ASM International, p 248
5. Dupasquier A, Ferragut R, Folegali P, Massazza M, Riontino G, Somoza A (2002) *Materials Science Form* 396–402:783
6. Macchi CE, Somoza A, Dupasquier A, Polmear IJ (2003) *Acta Mater* 51:5151
7. Riontino G, Massazza M (2004) *Phil Mag* 84:967
8. Lumley RN, Polmear IJ, Morton AJ (2005) *Mater Sci Techn* 21:1025
9. Lumley RN, Polmear IJ, Morton AJ (2002) *Mater Sci Form* 396–402:893
10. Lumley RN, Morton AJ, Polmear LJ (2002) *Acta Mater* 50:3597
11. Buha J, Lumley RN, Munroe PR, Crosky AG (2004) In: Nie JF, Morton AJ, Muddle BC (eds) *Proceedings of 9th international conference on aluminium alloys*. Brisbane, Australia, p 1167
12. Starink MJ, Sinclair I, Gao N, Kamp N, Gregson PJ, Pitcher PD, Levers A, Gardiner S (2002) *Mater Sci Form* 396–402:601
13. Gao N, Starink MJ, Davin L, Cerezo A, Wang S, Gregson PJ (2005) *Mater Sci Techn* 21:1010
14. Starink MJ (2004) *Int Mater Rev* 49:191
15. Starink MJ, Wang SC (2003) *Acta Mater* 51:5131
16. Kamp N, Starink MJ, Sinclair I, Gao N, Gregson PJ, Pitcher PD, Gardiner S (2004) In: Nie JF, Morton AJ, Muddle BC (eds) *Proceedings of 9th international conference on aluminium alloys*. Brisbane, Australia, p 369
17. Fang KT, Wang Y (1994) *Number-theoretic methods in statistics*. Chapman and Hall, London
18. Li R, Lin DKJ, Chen Y (2004) *Int J Materials Product Technol* 20:101
19. Fang KT (1980) *Acta Math Appl Sin* 3:362
20. Starink MJ, Yan J (2003) In: Tiryakioglu M, Lalli LA (eds) *Proceedings of ASM Materials Solutions Conference 2003, 1st International Symposium on Metallurgical Modeling for Al Alloys*. Pittsburgh, USA, p 119
21. Kamp N, Gao N, Starink MJ, Sinclair I (2004) Unpublished Research Report, University of Southampton
22. Starink MJ, Cerezo A, Yan JL, Gao N (2006) *Phil Mag Lett* 86:243
24. Wang SC, Starink MJ, Gao N (2006) *Scr Mater* 54:287
25. Yan J (2004) MPhil/PhD Transfer Thesis, University of Southampton, UK
26. Massazza M, Riontino G (2002) *Phil Mag Lett* 82:495